Elsevier Editorial System(tm) for Scripta Materialia

Manuscript Draft

Manuscript Number: SMM-15-1454R1

Title: Toughened and strengthened silicon carbide ceramics by adding graphene-based fillers

Article Type: Regular article

Keywords: graphene; ceramic matrix composites (CMC); mechanical properties; toughness; fracture

Corresponding Author: Dr. Manuel Belmonte,

Corresponding Author's Institution: Instituto de Cerámica y Vidrio

First Author: Manuel Belmonte

Order of Authors: Manuel Belmonte; Andres Nistal; Pierre Boutbien; Benito Roman-Manso; Isabel Osendi; Pilar Miranzo

Abstract: Graphene nanoplatelets and reduced graphene oxide (rGO) were selected as fillers to develop reinforced silicon carbide (SiC)/graphene composites. The mechanical properties of the materials were investigated as a function of the type of graphene source and graphene content. Composites containing just 5 vol.% of rGOs exhibited an outstanding mechanical performance, increasing both the fracture toughness in ~162%, with a maximum value of 8.3 MPa·m1/2, and the strength in ~ 60% (600 MPa) when compared to monolithic SiC . The preferential alignment of the graphene fillers, their dimensions, and the graphene-SiC mechanical interlock are key factors to promote crack shielding mechanisms.

*Manuscript (Text only)
Click here to view linked References

Toughened and strengthened silicon carbide ceramics by adding graphene-based fillers

M. Belmonte*, A. Nistal, P. Boutbien, B. Román-Manso, M. I. Osendi, P. Miranzo

Institute of Ceramics and Glass (ICV-CSIC) Campus Cantoblanco, c/Kelsen 5, 28049 Madrid, Spain

Abstract

Graphene nanoplatelets and reduced graphene oxide (rGO) were selected as fillers to develop reinforced silicon carbide (SiC)/graphene composites. The mechanical properties of the materials were investigated as a function of the type of graphene source and graphene content. Composites containing just 5 vol.% of rGOs exhibited an outstanding mechanical performance, increasing both the fracture toughness in ~162%, with a maximum value of 8.3 MPa·$m^{1/2}$, and the strength in ~ 60% (600 MPa) when compared to monolithic SiC . The preferential alignment of the graphene fillers, their dimensions, and the graphene-SiC mechanical interlock are key factors to promote crack shielding mechanisms.

Keywords: graphene; ceramic matrix composites (CMC); mechanical properties; toughness; fracture

Silicon carbide (SiC) is one of the most demanded engineering ceramics due to their excellent corrosion and wear resistances, jointly with a high thermal conductivity

*Author to whom correspondence should be addressed. E-mail: mbelmonte@icv.csic.es

and good mechanical performance at high temperature [1]. However, the Achilles' heel of these ceramics is their relatively low toughness. To overcome this problem, different approaches have been employed in the past for enhancing the fracture toughness (K_{IC}), among others, by inducing the in-situ growth of elongated SiC grains through thermal treatments (the so-called in-situ toughened SiC [2]) or by developing carbon fibre- or SiC fibre-reinforced SiC composites [3,4]. In both approaches, the fibres or the elongated grains deflect and/or bridge the cracks, arresting them or at least limiting their growth.

Recently, graphene-based nanostructures have attracted a great interest as efficient reinforcement fillers for toughening some oxide and non-oxide ceramics due to their capability for promoting toughening mechanisms [5-14]. Alumina (Al_2O_3)/graphene and silicon nitride (Si_3N_4)/graphene composites are the most investigated systems, and for which the most remarkable K_{IC} results have been obtained until now. Focusing on the Al_2O_3-based composites, Lee et al. [5] reported K_{IC} values up to 10.5 MPa·$m^{1/2}$ when 2 vol.% of reduced graphene oxide (rGO) was added, which corresponded to an increment of ~150% in this mechanical parameter as compared to the monolithic ceramics. Besides, the strength of the composite was also increased in 21%; whereas Centeno et al. [6] found improvements in σ of up to 80% for 0.22 wt.% rGOs composites, suggesting that the restriction of the Al_2O_3 grain growth during the sintering process due to the presence of graphene is the cause of that increment. In the case of Si_3N_4/graphene composites, a toughness increase of 135% was reported by Walker at al. [7] and Ramirez et al. [8]. The latter authors reached a maximum K_{IC} value of 10.4 MPa·$m^{1/2}$ when 4.3 vol.% rGOs were added to the Si_3N_4 matrix, jointly with an augment in σ of 10% (maximum value of 1050 MPa) [8]. Other ceramics have been explored in this sense (for graphene reinforcement) with dissimilar results. For

example, Shin et al. [9] increased the fracture toughness of yttria-stabilized zirconia (YSZ) ceramics in ~ 34% by adding 4 vol.% of rGOs; while Nieto et al. [10] reached K_{IC} improvements of ~ 100% for tantalum carbide (TaC) ceramics with 5 vol.% of graphene nanoplatelets (GNPs), attaining top K_{IC} values of 11.7 MPa·$m^{1/2}$. Yun et al. [11] recently reported the mechanical performance of aluminium nitride (AlN)/1.5 vol.% GNPs composites, showing increases on K_{IC} and σ of about 30% and 17%, respectively. In the case of SiC ceramics, some of the present authors pioneered the manufacturing of SiC/graphene composites by the in-situ growth of graphene sheets (~ 3-4 vol.%) into bulk SiC ceramics during the spark plasma sintering (SPS) process [12], which improved both the fracture toughness in ~55% [12] and the resistance to cone/ring cracking under Hertzian contact stresses [13]. Lately, Rahman et al. [14] reported a 40% K_{IC} improvement when adding 2 wt.% of GNPs to a polymer SiC precursor, despite the remaining porosity in the composites.

The aim of this work is to investigate the fracture toughness and strength performances of dense SiC ceramics as a function of the GNPs content and the type of graphene source, in particular, comparing the mechanical properties attained with different graphene fillers, such as GNPs, rGOs -from in-situ reduced GOs during SPS-, and finally, graphene epitaxially grown in-situ within the SiC ceramics.

GO nanoplatelets (< 5 nm thickness, < 5 μm x-y dimensions), prepared in in-house from graphite flakes using the modified Hummers method [15], and commercial GNPs (Angstron Materials Inc., USA, nominal thickness and x-y dimensions of 10-20 nm and 14 μm, respectively) were selected as fillers. SiC/graphene composites were prepared as detailed next. Firstly, graphene fillers were sonicated in alcohol -ethanol for GOs and isopropyl alcohol for GNPs- for 1 h and, meanwhile, an alcohol-based ceramic slurry containing 93 wt.% of β-SiC powders (BF-17A, H.C. Starck, Germany) plus 5

wt.% of Y_2O_3 (Grade C, H.C. Starck, Germany) and 2 wt.% of Al_2O_3 (SM8, Baikowski Chimie, France), both used as sintering additives, was attrition milled for 2 h. Both suspensions were blade mixed and sonicated for 1 h, dried at 120 °C, and sieved through a 63 μm mesh. The following compositions were prepared: monolithic; 5 vol.% of GOs, and 5, 10 and 20 vol.% of GNPs. Finally, disc shaped specimens of 20 mm × 3 mm were SPSed (Dr. Sinter, SPS-510CE, Japan) at 1800 ºC for 5 min, applying a uniaxial pressure of 50 MPa during the heating cycle, and using a vacuum atmosphere of ~6 Pa. Apparent density was measured by the water immersion method. The different materials were characterized by field emission scanning electron microscopy (FESEM, S-4700, Hitachi, Japan) and micro-Raman spectroscopy (Alpha300 WITec GmbH, Germany) using the 532 nm laser wavelength excitation. Median grain diameter (d_{50}) and aspect ratio (AR_{50}) of the SiC matrix were quantified by imaging analysis methods on FESEM micrographs taken on polished and plasma etched surfaces, and considering at least 500 features. For the mechanical tests small bars of 15.0 mm x 2.0 mm x 2.5 mm were prepared. Flexural strength (σ) was determined by three point bending tests using an outer span of 8 mm and a displacement rate of 0.5 $mm \cdot min^{-1}$. Fracture toughness (K_{IC}) was measured by the surface crack in flexure (SCF) method by Knoop indenting at 100 N the centre of the bars in their tensile surfaces and, then, performing three point bending tests with the same outer span and displacement rate than for σ. At least four bars were tested per material and mechanical parameter. Besides, to observe in detail the crack paths, Vickers indentations at loads ranging from 20 to 100 N were performed at the cross section of the bars that corresponded to the plane parallel to the SPS pressing axis.

Highly homogenous and fully dense β-SiC materials were obtained, where the graphene fillers appeared preferentially oriented with their ab plane perpendicular to the SPS pressing axis (Fig. 1). The reference monolithic material also contained ~ 3-4 vol.% of graphene multilayers (Fig. 1a), which were grown in-situ at the SiC grain boundaries during the SPS process [12]. GNPs remained undamaged after the SPS process, as the intensity ratio between D and G Raman bands (I_D/I_G) slightly increased, i.e., the GNPs become more defective, changing from 0.21 for the pristine GNPs to 0.23-0.28 after the sintering step. Conversely, I_D/I_G for GOs considerably decreased from 1.20 (as-produced) to 0.29 (after SPS), which constitutes a proof of the effective reduction of GO (rGO) to graphene by the SPS method [16]. Regarding the microstructure, it should be noticed that all the materials presented the same matrix grain size and shape (d_{50} = 0.6-0.7 μm and AR_{50} = 1.4).

The strength and fracture toughness data as a function of the graphene source are plotted in Fig. 2a,b. At first glance, the graphene composites exhibited better mechanical performance than the reference material. In this way, the strength of SiC ceramics increased in ~ 60-70% when 5 vol.% of fillers either GNPs or rGOs were added to the matrix (Fig. 2a), reaching a maximum σ value of 622 MPa for the GNPs composite. Furthermore, almost no differences (< 4%) in the strength were observed when varying the graphene source. The strengthening of the graphene composites is quite remarkable considering that the matrix grain size remains unchanged and much smaller, about one order of magnitude, than the maximum lateral filler size (< 5 and 14 μm for GOs and GNPs, respectively), which, therefore, controls the critical flaw size. Accordingly, the observed strengthening should be linked to an expected toughness increase in the composites, as presently occurred in all composites and shown in Fig. 2b. In fact, rGOs led to an outstanding increase in K_{IC} (8.3 $MPa \cdot m^{1/2}$) with respect to

monolithic SiC (3.2 MPa·$m^{1/2}$) that corresponded to a toughness increment of 162%. Interestingly, this K_{IC} value is one of the highest toughness data reported for SiC materials, with the exception of some three dimensional textile C/SiC and SiC/SiC composites with K_{IC} over 20 MPa·$m^{1/2}$ [1], being also remarkable the low reinforcing phase content (5 vol.% rGOs) required to achieve these results. Comparing to other ceramic/graphene composites, this exceptional K_{IC} improvement is even higher than that for Al_2O_3/rGOs [5] and Si_3N_4/rGOs composites [7,8]. The benefits of adding GNPs are less pronounced, as a lower K_{IC} value was assessed (4.8 MPa·$m^{1/2}$), although these nanoplatelets still promoted a significant toughness enhancement of 50% as compared to monolithic SiC. Finally, the monolithic material exhibited a K_{IC} value (3.2 MPa·$m^{1/2}$) just slightly higher than that reported by Borrero-Lopez et al. [17] for hot pressed SiC ceramics (K_{IC} = 2.9 MPa·$m^{1/2}$) with a similar amount of sintering additives and grain size to the present case but without graphene fillers. Despite the current monolithic material already contained ~3-4 vol.% of graphene multilayers in-situ grown, their random distribution within the matrix contributed less to the development of toughening mechanisms.

FESEM observations of Vickers indentation imprints performed in the plane parallel to the SPS pressing axis (Fig. 3), i.e., perpendicular to the plane containing the oriented graphene sheets, clearly illustrate that well-defined vertical and horizontal cracks were developed in the reference material (Fig. 3a). However, for SiC/graphene composites, especially that containing rGOs (Fig. 3b), vertical cracks are mostly horizontally deflected, propagating freely in that direction. A FESEM image at higher magnification of one of the short vertical cracks reveals the reason for their arresting (Figs. 3c,d). As it can be seen, extrinsic crack-tip-shielding mechanisms associated to GNPs (Fig. 3c) and rGOs sheets (Fig. 3d) effectively bridged the crack, thus reducing

the local stresses and strains at the crack tip and, hence, inhibiting the crack growth and enhancing the toughness of the composite [18]. Crack deflection is also evidenced in the indentation cracks, as shown by the brisk change in crack direction when impinging the graphene planes, which produces mix-mode crack propagation that also results in a reinforcing effect. These toughening mechanisms are particularly favoured in the vertical direction because the ab planes of the graphene fillers are mostly oriented perpendicular to that direction. Conversely, those mechanisms were not as effective when the horizontal cracks run parallel to the ab planes of the fillers. The superior toughness achieved for the rGOs composite (Fig. 2b) could be explained attending to several reasons. First, rGOs are smaller and thinner than GNPs and, hence, for the same volume fraction, the number of potential graphene-based ligaments to bridge the cracks would be higher in the case of rGOs. In addition, these graphene fillers may exhibit a certain mechanical interlock with the matrix, as they appear wavy following boundaries of the SiC grains (pointed by arrows in Fig. 1b), which would result in a larger energy consumption when rGOs are debonded by the cracks [19].

The role of the graphene filler content on the mechanical parameters has been evaluated in the composites containing GNPs (Figs. 2c,d). These nanoplatelets were chosen, instead rGOs, because their higher availability and also considering that they produced reasonable toughening and strengthening effects. Regarding the flexure strength (Fig. 2c), the response was better for any composite as compared to monolithic SiC, even for materials containing up to 20 vol.% of GNPs (8% increase in σ). Despite the maximum σ value was attained for SiC/5 vol.% GNPs composite (622 MPa, 67% improvement), the strength just slightly decreased (602 MPa) when the amount of GNPs was doubled (10 vol.%). For larger nanoplatelets contents, a percolated graphene network is formed that leads to an increased critical flaw size, decreasing the strength of

the material. Interestingly, the fracture toughness increased for materials containing up to 10 vol.% of GNPs (Fig. 2d) to a value of 5.9 MPa·$m^{1/2}$ that represents an improvement of 86% as compared to the monolithic material. Fig. 4a-c are clear examples of the multiple bridging, branching and deflection events occurring in indentation cracks propagating in the vertical direction, which led to their arresting. However, when cracks propagate along the parallel direction with respect to the ab plane of the GNP, the nanoplatelets are mostly delaminated and exfoliated (Fig. 4d). Similarly to the strength plot, toughness values dropped for GNPs contents of 20 vol.% because the formed graphene network weakens the material, controls its failure and stabilizes the contribution of bridging mechanisms [19].

In summary, toughened and strengthened SiC ceramics are developed incorporating graphene fillers to the ceramic matrix. Reduced GOs arise as the best graphene filler considering the outstanding toughness increment (162%) and strength up to ~ 600 MPa (61%) attained by adding just 5 vol.% of rGOs to the ceramic matrix. The lower dimensions and the better mechanical interlock to the matrix of rGOs, when compared to GNPs, support the excellent mechanical performance of SiC/rGOs composites. In the case of GNPs composites, filler contents up to 10 vol.% are required to potentially promote a larger occurrence of crack shielding mechanisms and a maximum toughness increase of 86%, while keeping a constant strength value around 600 MPa.

Acknowledgements

This work was supported by the Spanish Government and CSIC under projects MAT2012-32944 and PIE201360E063, respectively.

References

[1] K.A. Schwetz, Silicon carbide based hard materials - Handbook of ceramic hard materials, Wiley Online Library, Weinhein, 2008.

[2] N.P. Padture, J. Am. Ceram. Soc. 77 (1994) 519.

[3] Y Xu, L. Cheng, L. Zhang, H. Yin, X. Yin, Mater. Sci. Eng. A 300 (2001) 196.

[4] C. Droillard, J. Lamon, J. Am. Ceram. Soc. 79 (1996) 849.

[5] B. Lee, M.Y. Koo, S.H. Jin, K.T. Kim, S.H. Hong, Carbon 78 (2014) 212.

[6] A. Centeno, V.G. Rocha, B. Alonso, A. Fernandez, C.F. Gutierrez-Gonzalez, R. Torrecillas, A. Zurutuza, J. Eur. Ceram. Soc. 33 (2013) 3201.

[7] L.S. Walker, V.R. Marotto, M.A. Rafiee, N. Koratkar, E.L. Corral, ACS Nano 5 (2011) 3182.

[8] C. Ramirez, P. Miranzo, M. Belmonte, M.I. Osendi, P. Poza, S.M. Vega-Diaz, M. Terrones, J. Eur. Ceram. Soc. 34 (2014) 161.

[9] J.H. Shin, S.H. Hong, J. Eur. Ceram. Soc. 34 (2014) 1297.

[10] A. Nieto, D. Lahiri, A. Agarwal, Mater. Sci. Eng. A 582 (2013) 338.

[11] C. Yun, Y. Feng, T. Qiu, J. Yang, X. Li, L. Yu, Ceram. Int. 41 (2015) 8643.

[12] P. Miranzo, C. Ramirez, B. Roman-Manso, L. Garzon, H.R. Gutierrez, M. Terrones, C. Ocal, M.I. Osendi, M. Belmonte, J. Eur. Ceram. Soc. 33 (2013) 1665.

[13] B. Roman-Manso, E. Sanchez-Gonzalez, A.L. Ortiz, M. Belmonte, M.I. Osendi, P. Miranzo, J. Eur. Ceram. Soc. 34 (2014) 1433.

[14] A. Rahman, A. Singh, S. Karumuri, S.P. Harimkar, K.A. Kalkan, R.P. Singh, Composite, Hybrid, and Multifunctional Materials 4 (2015) 199.

[15] S. Gilje, S. Han, M. Wang, K.L. Wang, R.B. Kaner, Nano Lett. 7 (2007) 3394.

[16] C. Ramirez, S.M. Vega-Diaz, A. Morelos-Gomez, F.M. Figueiredo, M. Terrones, M.I. Osendi, M. Belmonte, P. Miranzo, Carbon 57 (2013) 425.

[17] O. Borrero-Lopez, A.L. Ortiz, F. Guiberteau, N.P. Padture NP, J. Eur. Ceram. Soc. 27 (2007) 3351.

[18] R.O. Ritchie RO, Nat. Mater. 10 (2011) 817.

[19] C. Ramirez, M.I. Osendi, Ceram. Int. 40 (2014) 11187.

Figure captions

Figure 1. FESEM micrographs of the fracture surface corresponding to the different materials: a) monolithic SiC materials containing graphene multilayers grown in-situ, and composites containing: b) 5 vol.% rGOs, c), 5 vol.% GNPs, d) 10 vol.% GNPs, and e) 20 vol.% GNPs (e). Arrows in (a) and (b) point graphene multilayers in-situ formed in SiC and rGOs showing waviness, respectively.

Figure 2. a) and c) Flexure strength, σ, and b) and d) fracture toughness, K_{IC}, for SiC/graphene composites: a) and b) containing a fixed amount (5 vol.%) of different graphene sources, and c) and d) varying the GNPs content.

Figure 3. FESEM micrographs of the cracks developed by Vickers indentation at 100 N on the plane parallel to the SPS pressing axis of the materials: a) and b) imprints performed in monolithic SiC and 5 vol.% rGOs composite, respectively. Toughening mechanisms events are observed in composites containing 5 vol.% of: c) GNPs and d) rGOS.

Figure 4. FESEM micrographs of the cracks developed by Vickers indentation at 100 N for SiC composites containing: a,b) 10 vol.% GNPs and c,d) 20 vol.% GNPs. In a-c) the cracks run in the plane parallel to the SPS pressing axis; whereas in d) they run in the perpendicular plane.

Figure 1

Click here to download high resolution image

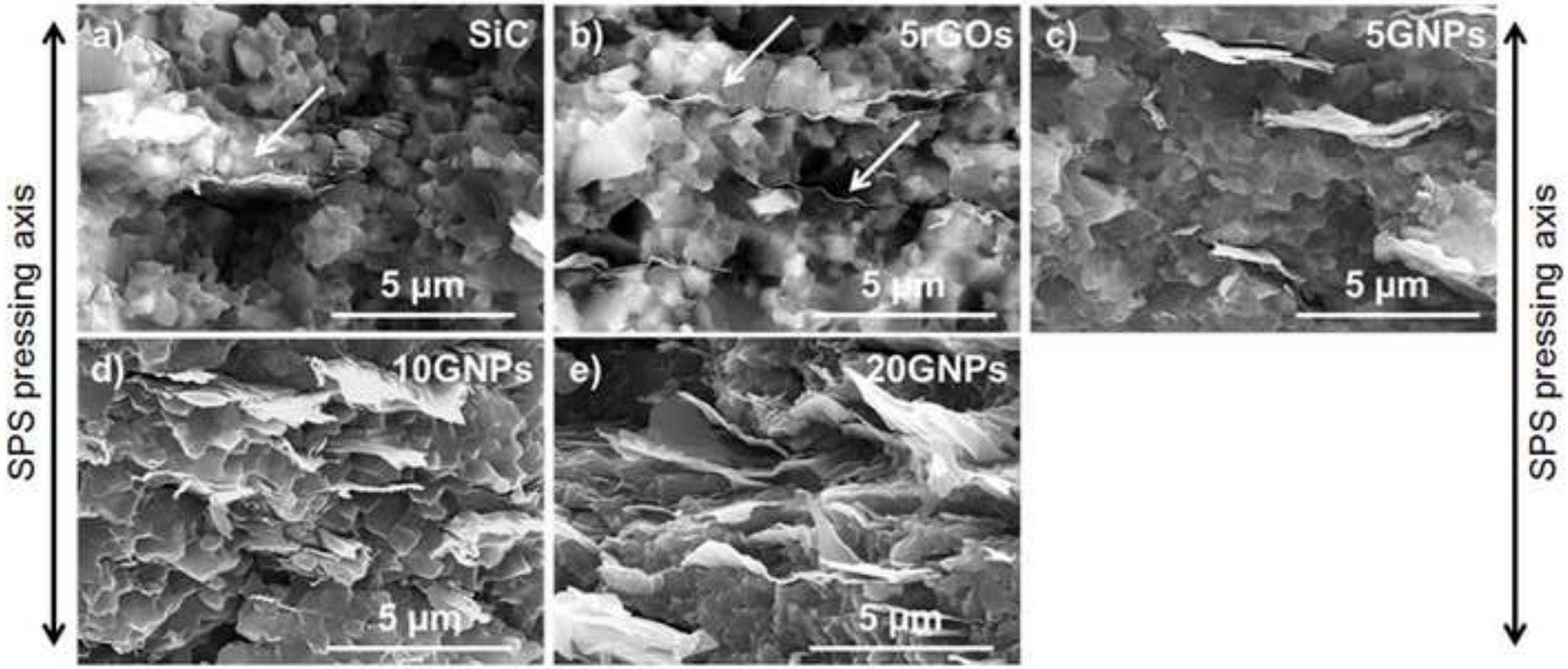

Figure 2

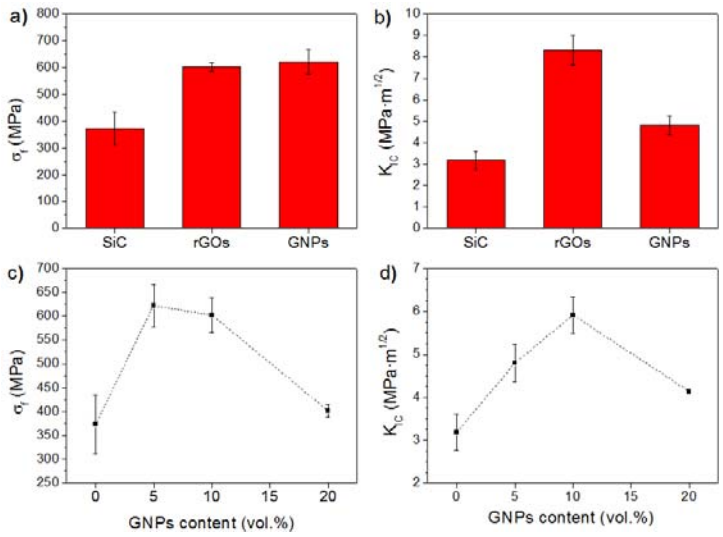

Figure 3

Click here to download high resolution image

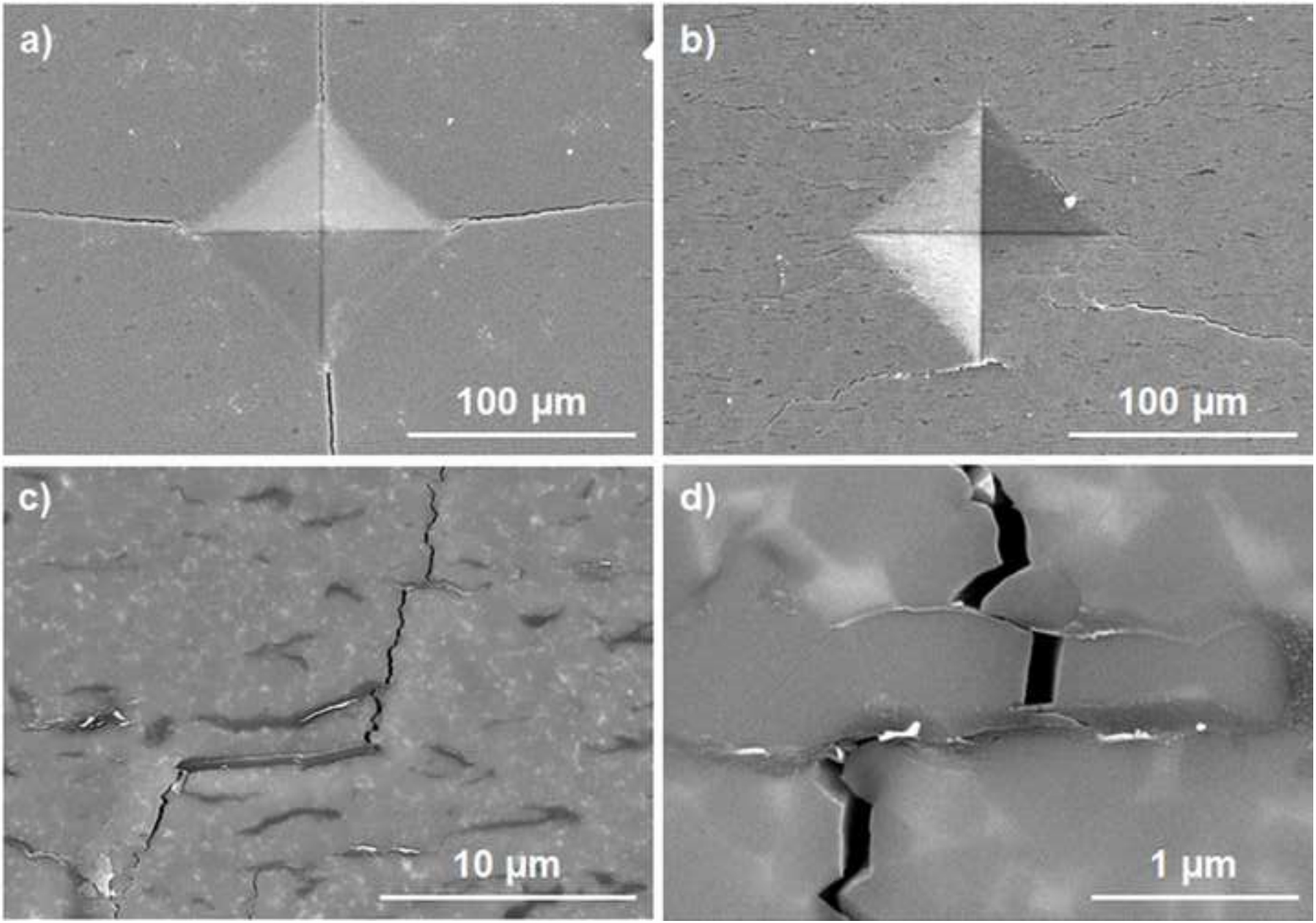

Figure 4

Click here to download high resolution image